Supporting Information for

Rapid topographic growth of the Diancang Shan, southeastern margin of the Tibetan Plateau since 5.0–3.5 Ma

Chunxia Zhang[1,2], Haibin Wu[1,3], Xiuli Zhao[2], Yunkai Deng[1,3], Yunxia Jia[4], Wenchao Zhang[1], Shihu Li[5], Chenglong Deng[3,5]

[1]Key Laboratory of Cenozoic Geology and Environment, Institute of Geology and Geophysics, Chinese Academy of Sciences, Beijing 100029, China

[2]College of Earth Science and Engineering, Shandong University of Science and Technology, Qingdao 266590, Shandong Province, China

[3]University of Chinese Academy of Sciences, Beijing, China

[4]School of Geographical Science, Shanxi Normal University, Taiyuan 030031, China

[5]State Key Laboratory of Lithospheric Evolution, Institute of Geology and Geophysics, Chinese Academy of Sciences, Beijing 100029, China

Correspondence to: Chunxia Zhang (cxzhang@mail.iggcas.ac.cn)

Contents of this file

Introduction

This supplementary material contains one section of text (Text S1), one supplementary figure (Figure S1), and two tables (Table S1, S2).

Text S1

Climate reconstruction method base on pollen data

The Modern Analogue Technique (MAT) is a commonly used method for reconstructing past climate (Overpeck et al., 1985). This approach was based on the measure of the degree of similarity between fossil pollen and modern pollen (Chevalier et al., 2020).

This analogue-based approach avoided to fit the pollen-climate models, thus outperformed other regression-based approach (such as weighted averaging-partial least squares, WAPLS) (ter Braak and Juggins, 1993; Zhang et al., 2022). However, this approach might suffer from the so-called ‘no-analogue’ problem (Chevalier et al., 2020). The pollen taxa-PFT transformation scheme was later developed to address this problem (Peyron et al., 1998). The plant function types (PFTs) are groups of plants characterized by common phenological and climate constraints, thus the taxa with no modern analog can be replaced by other taxa within the same PFT group (Mauri et al., 2015; Prentice et al., 1992). The PFT-based MAT method has been widely employed in the paleoclimate reconstruction (Davis et al., 2003; Peyron et al., 1998; Zhang et al., 2022).

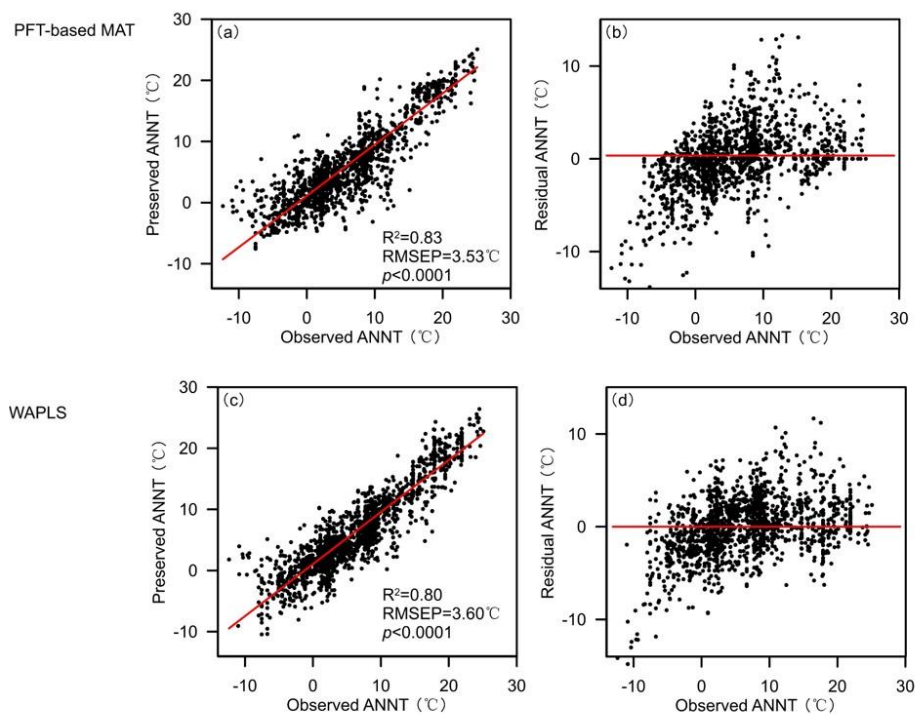

Figure S1. Scatter plots and residuals of observed vs. predicted *ANNT* based on PFT-based Modern Analogue Technique (MAT, k=6) and weighted-average partial least squares (WAPLS, component=3) estimated by bootstrapping cross-validation.

Table S1. The thickness, lithology of samples for pollen analyses, and the total sum of pollen grains for each sample.

Thickness (m)	Lithology	Pollen grain's sum	Thickness (m)	Lithology	Pollen grain's sum
965	Silt clay	274	536	Conglometare, sandstone	0
954	Shallow-yellow siltstone	0	**525**	Silt clay	333
943	Shallow-yellow sandstone	2	512	Sandstone	0
953	Shallow-yellow siltstone	0	**503**	Silt clay	317
924		0	492	Siltstone	0
910		0	**481**	Silt clay	320
899	Gray silt clay	325	470	Siltstone	0
865	Conglometare, sandstone	0	**459**	Silt clay	287
855	Silt clay	270	448	Red sandstone	0
844	Gray silt clay	344	437	Red siltclay, siltstone	0
833		291	426		0
820	Conglometare, sandstone	0	415		1
811	Siltstone	310	405		1
800	Light-red siltsone	317	395		0
789	Red siltsone	0	385	Red siltstone	0
778	Light-red siltsone	355	370		0
777		288	339		0
767	Gray sandstone	0	338		0
756	Light-red siltsone	296	322	Red siltclay	0
745	Gray sandstone	0	314.6		0
734		0	**291.6**	Peat clay, coal	417
721		0	**258.6**		346
711		0	**248.6**		305
701	Silt clay	302	**223.6**		530
690	Siltstone	0	196.6	Yellow sandstone	0
679		0	189.6		0
668	Silt clay	277	183.6		0
657		296	**174.6**	Peat clay, coal	334
646	Siltstone	0	**170.6**		350
635	Sandstone	0	**169.6**		350
624	Silt clay	305	**168.6**		268
613	Siltsone	0	**155.6**		364
604		0	**146.6**		354
590	Silt clay	289	**144.6**		452
580	Conglometare, sandstone	0	123.6	Sandstone	0
569		0	113.6		0
547	Silt clay	289	103.6		0

Table S2. Thermochronological data from the eastern and southern margins of DCS

Site	Age (Ma)	Range	Mineral	Reference
Southern margin of DCS	4.3	0.1	K-feldspar	(Leloup et al., 1993)
	4.5	-		
	5.0	-		
	4.5	-		
	4.7	-		
	4.5	-		
	5.97	0.04	K-feldspar	(Cao et al., 2011)
	4.34	0.13		
	5.0	-		
	5.74	0.2		
	7.0	-		
	4.58	0.15		
	7.64	0.04		
	5.1	0.27		
	6.44	0.14	Biotite	
	6.4	0.3		
Eastern margin of DCS	6.6	1.3	Biotite	(Li et al., 2012)
	5.9	0.4	K-feldspar	
	4.21	0.02	Apatite	
	3.48	0.17		
	3.99	0.13		
	3.59	0.06		
	4.4	0.11		
	5.96	0.82		
	4.67	0.57		
	6.44	0.05		
	5.22	0.42		
	5.54	1.25		
	5.44	0.96		
	7.72	0.54		
	8.22	0.09		
	6.47	1.02		
	4.15	2.65		
	5.82	0.44		
	6.02	0.12		
	4.28	0.02		
	3.53	0.17		
	4.04	0.13		
	3.63	0.06		
	4.46	0.11		
	6.07	0.82		
	4.8	0.57		

	6.52	0.05		
	5.36	0.43		
	5.71	1.26		
	5.59	0.96		
	7.83	0.55		
	3.79	0.09		
	6.63	1.03		
	8.74	0.11		
	4.44	-		
	6.1	0.44		
	2.72	0.47	Illite	(Han et al., 2011)

References

Cao, S.Y., Neubauer, F., Liu, J.L., Genser, J.& Leiss, B. (2011). Exhumation of the Diancang Shan metamorphic complex along the Ailao Shan-Red River belt, southwestern Yunnan, China: Evidence from $^{40}Ar/^{39}Ar$ thermochronology. *Journal of Asian Earth Sciences*, 42, 525-550.

Chevalier, M., Davis, B.A.S., Heiri, O. et al. (2020). Pollen-based climate reconstruction techniques for late Quaternary studies. *Earth-Science Reviews*, 210, 103384.

Davis, B.A.S., Brewer, S., Stevenson, A.c.& Guiot, J. (2003). The temperature of Europe during the Holocene reconstructed from pollen data. *Quaternary Science Reviews*, 22, 1701-1716.

Fan, C., Wang, G., Wang, S.F.& Wang, E. (2006). Structural interpretation of extensional deformation along the Dali fault system, southeastern margin of the Tibetan plateau. *International Geology Review*, 48(4), 287-310.

Han, S.Q., Chen, Q.L.& Zhang, Y.S. (2011). K-Ar age of authigenic illite in fault gouge in the northern section of Red River fault and geological significance (in Chinese). *Quaternary Sciences*, 27(6), 1129-1130.

Leloup, P.H., Harrison, T.M., Ryerson, F.J. et al. (1993). Structural, petrological and thermal evolution of a tertiary ductile strike-slip shear zone, Diancong shan, Yunnan. *Journal of Geophysical Research*, 98(B4), 6715-6743.

Li, B.L., Ji, J.Q., Lo, C.H., Gong, J.F.& Qing, J.C. (2012). The structural style and timing of uplift of the Ailao Shan- Diancang Range, West Yunnan, China (in Chinese with English abstract). *Seismology and Geology*, 34(4), 696-712.

Liu, J., Tang, L., Qiao, Y., Head, M.J.& Walker, D. (1986). Late Quaternary vegetation history at Menghai, Yunnan province, southwest China. *Journal of Biogeography*, 13, 399-418.

Mauri, A., Davis, B.A.S., Collins, P.M.& Kaplan, J.O. (2015). The climate of Europe during the Holocene: a gridded pollen-based reconstruction and its multi-proxy evaluation. *Quaternary Science Reviews*, 112, 109-127.

Ming, T.L.& Fang, R.Z. (1982). The vegetation on Cangshan Yunnan and the distribution of genus Rhododendron (in Chinese with English abstract). *Acta Botanica Yunanica*, 4(4), 383-391.

Overpeck, J.T., Webb, T.& Prentice, I.C. (1985). Quantitative interpretation of fossil pollen spectra: Dissimilarity coefficients and the method of modern analogs. *Quaternary Research*, 23(1), 87-108.

Peyron, O., Guiot, J., Cheddadi, R. et al. (1998). Climatic Reconstruction in Europe for 18,000 YR B.P. from Pollen Data. *Quaternary Research*, 49(2), 183-196.

Prentice, I.C., Cramer, W., Harrison, S.P. et al. (1992). Special Paper: A Global Biome Model Based on Plant Physiology and Dominance, Soil Properties and Climate. *Journal of Biogeography*, 19(2).

Shen, J., Jones, R.T., Yang, X.D., Dearing, J.A.& Wang, S.M. (2006). The Holocene vegetation history of Lake Erhai, Yunnan province southwestern China: the role of climate and human forcings. *The Holocene*, 16(2), 265-276.

Sun, A.Z., Luo, Y.L., Wu, H.B. et al. (2020). An updated biomization scheme and vegetation reconstruction based on a synthesis of modern and mid-Holocene pollen data in China. *Global and Planetary Change*, 192, 103178.

ter Braak, C.J.F.& Juggins, S. (1993). Weighted averaging partial least squares regression (WA-PLS): an improved method for reconstructing environmental variables from species assemblages. *Hydrobiologia*, 269(1), 485-502.

Zhang, W.C., Wu, H.B., Cheng, J. et al. (2022). Holocene seasonal temperature evolution and spatial variability over the Northern Hemisphere landmass. *Nature Communications*, 13(1), 5334.